

AD-A268 203



2

ARMY RESEARCH LABORATORY



# Effect of Molybdenum Ion Implantation on the Pitting Corrosion of Depleted Uranium - 0.75 Titanium Alloy

K.-S. Lei, F. Chang, and M. Levy

ARL-TR-144

July 1993

DTIC  
ELECTE  
AUG 12 1993  
S B D

Approved for public release; distribution unlimited.

93-18860



1385

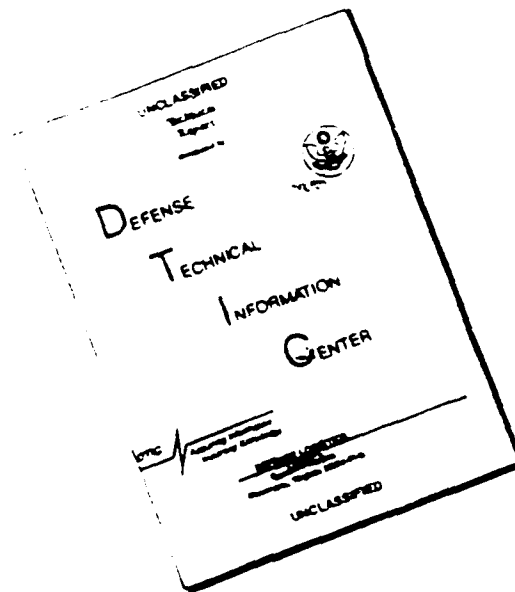
93

The findings in this report are not to be construed as an official Department of the Army position unless so designated by other authorized documents.

Citation of manufacturer's or trade names does not constitute an official endorsement or approval of the use thereof.

Destroy this report when it is no longer needed. Do not return it to the originator.

# DISCLAIMER NOTICE



THIS DOCUMENT IS BEST QUALITY AVAILABLE. THE COPY FURNISHED TO DTIC CONTAINED A SIGNIFICANT NUMBER OF PAGES WHICH DO NOT REPRODUCE LEGIBLY.

REPORT DOCUMENTATION PAGE			Form Approved OMB No. 0704-0188	
Public reporting burden for this collection of information is estimated to average 1 hour per response, including the time for reviewing instructions, searching existing data sources, gathering and maintaining the data needed, and completing and reviewing the collection of information. Send comments regarding this burden estimate or any other aspect of this collection of information, including suggestions for reducing this burden, to Washington Headquarters Services, Directorate for Information Operations and Reports, 1215 Jefferson Davis Highway, Suite 1204, Arlington, VA 22202-4302, and to the Office of Management and Budget, Paperwork Reduction Project (0704-0188), Washington, DC 20503.				
1. AGENCY USE ONLY (Leave blank)		2. REPORT DATE July 1993		3. REPORT TYPE AND DATES COVERED Final Report - Reprint
4. TITLE AND SUBTITLE Effect of Molybdenum Ion Implantation on the Pitting Corrosion of Depleted Uranium - 0.75 Titanium Alloy			5. FUNDING NUMBERS	
6. AUTHOR(S) K.-S. Lei,* F. Chang, and M. Levy				
7. PERFORMING ORGANIZATION NAME(S) AND ADDRESS(ES) U.S. Army Research Laboratory Watertown, MA 02172-0001 ATTN: AMSRL-MA-MA			8. PERFORMING ORGANIZATION REPORT NUMBER  ARL-TR-144	
9. SPONSORING/MONITORING AGENCY NAME(S) AND ADDRESS(ES) U.S. Army Research Laboratory 2800 Powder Mill Road Adelphi, MD 20783-1145			10. SPONSORING/MONITORING AGENCY REPORT NUMBER	
11. SUPPLEMENTARY NOTES *Presently at Compaq Computer Corp., P.O. Box 692000, MS 060105, Houston, TX 97242. Published in Proceedings of the 2nd International Conference on Localized Corrosion, 1987, p. 459 to p. 465.				
12a. DISTRIBUTION/AVAILABILITY STATEMENT  Approved for public release, distribution unlimited.			12b. DISTRIBUTION CODE	
13. ABSTRACT (Maximum 200 words)  Pitting corrosion of molybdenum-ion-implanted, depleted uranium -0.75 Ti (DU -0.75 Ti) has been studied electrochemically in acidic, neutral, and alkaline solutions containing sodium chloride, and the results have been compared to those of the unimplanted DU -0.75 Ti. The data show that Mo implantation shifts the pitting potential of DU -0.75 Ti in the noble direction in acidic and alkaline solutions. In neutral 50 ppm Cl <sup>-</sup> solution, however, there is no beneficial effect of Mo implantation. Auger analysis studies show that before exposure to the solutions, all the molybdenum is in the oxide, which is approximately 1000 Å thick. After electrochemical scans in the acidic and alkaline chloride solutions, most of the Mo disappears from the oxide. However, no decrease in Mo concentration is found after exposure in neutral chloride solution. It is proposed that the implanted molybdenum dissolves in the acidic and alkaline solutions and forms simple or complex molybdates that inhibit pitting corrosion. The implanted molybdenum does not dissolve in the neutral chloride solution and inhibition does not occur.				
14. SUBJECT TERMS Uranium alloys, Uranium titanium alloys, Molybdenum, Ion implantation, Corrosion, Pitting, Surface inhabitation analysis			15. NUMBER OF PAGES 11	
			16. PRICE CODE	
17. SECURITY CLASSIFICATION OF REPORT Unclassified	18. SECURITY CLASSIFICATION OF THIS PAGE Unclassified	19. SECURITY CLASSIFICATION OF ABSTRACT Unclassified	20. LIMITATION OF ABSTRACT UL	

# Effect of Molybdenum Ion Implantation on the Pitting Corrosion of Depleted Uranium -0.75 Titanium Alloy

K.-S. Lei,\* F. Chang,\*\* and M. Levy \*\*

## Abstract

Pitting corrosion of molybdenum-ion-implanted, depleted uranium -0.75 Ti (DU -0.75 Ti) has been studied electrochemically in acidic, neutral, and alkaline solutions containing sodium chloride, and the results have been compared to those of the unimplanted DU -0.75 Ti. The data show that Mo implantation shifts the pitting potential of DU -0.75 Ti in the noble direction in acidic and alkaline solutions. In neutral 50 ppm  $\text{Cl}^-$  solution, however, there is no beneficial effect of Mo implantation. Auger analysis studies show that before exposure to the solutions, all the molybdenum is in the oxide, which is approximately 1000 Å thick. After electrochemical scans in the acidic and alkaline chloride solutions, most of the Mo disappears from the oxide. However, no decrease in Mo concentration is found after exposure in neutral chloride solution. It is proposed that the implanted molybdenum dissolves in the acidic and alkaline solutions and forms simple or complex molybdates that inhibit pitting corrosion. The implanted molybdenum does not dissolve in the neutral chloride solution and inhibition does not occur.

## Introduction

Depleted uranium (DU) has good ballistic properties but poor corrosion resistance in moist air and in salt-laden environments. Alloying depleted uranium with Ti, Mo, or Nb reduces the corrosion rate of pure DU.<sup>1-3</sup> However, these alloys are still susceptible to localized corrosion when chloride ions are present. Various coatings and surface treatments have been explored as protective schemes for uranium alloys.<sup>4-6</sup> Surface-modification techniques such as ion implantation offer several advantages, e.g., dimensional stability and good adhesion, while maintaining the bulk properties. Furthermore, this approach has been shown to increase the corrosion resistance of various alloy systems.<sup>7</sup> Thus, ion implantation may be a highly desirable method for providing not only corrosion resistance to DU but also maintaining the high density necessary for armor applications. This research effort studied the pitting corrosion resistance of DU -0.75 Ti after ion implantation of Mo<sup>+</sup> onto its surface. Electrochemical studies were conducted in acidic, neutral, and alkaline solutions containing sodium chloride. Electron dispersive spectroscopy (EDS) and Auger electron spectroscopy (AES) analyses were used to characterize the surface before and after exposure to these solutions. Experimental results of DU -0.75 Ti and Mo-implanted DU -0.75 Ti (Mo/DU -0.75 Ti) are compared and the possible mechanisms describing the effects of molybdenum implantation on pitting are discussed.

## Experimental

### Sample preparation

The DU -0.75 wt% Ti alloy used in this study was first melted

in a Varian<sup>†</sup> electric-arc furnace under vacuum ( $10^{-5}$  Torr) and cast into a cylindrical steel mold to form a rod of 1.0-in. (2.54-cm) diameter. The alloy was hot rolled, solution treated, water quenched, and aged. Samples of 5/8-in. (1.59-cm) diameter and 1/8-in. thickness were fabricated from the 1.0-in. rod. As indicated in the phase diagram, the equilibrium structure of DU -0.75 Ti consists of a major  $\alpha$  phase and a minor  $\text{U}_2\text{Ti}$  phase.<sup>8</sup> The alloy has a martensitic structure and a grain size of about 400  $\mu\text{m}$ .

### Ion implantation

The ion implantation was performed at the Naval Research Laboratory. After cleaning, the samples were implanted with 75 KeV Mo<sup>+</sup> ions to a dosage of  $6 \times 10^{16}$  ions/cm<sup>2</sup>, and then with 150 KeV Mo<sup>+</sup> ions to  $1.2 \times 10^{17}$  ions/cm<sup>2</sup>. This implantation procedure was intended to produce a Mo concentration profile such that the concentration of molybdenum (35 at%) remains constant at the first several hundreds of angstroms under the surface instead of the normal distribution type of concentration profile usually obtained by one-step implantation. But the actual composition profile displayed a normally distributed molybdenum as shown later.

### Electrochemical studies

Electrochemical measurements were performed using an EG&G Princeton Applied Research<sup>†</sup> (PAR) K0047 Corrosion Cell, a PAR 273 Potentiostat/Galvanostat, an Apple<sup>†</sup> IIe personal computer, and a PAR 332 Softcorr program. Solutions were made of reagent-grade chemicals and distilled water. Before testing, the solution was deaerated for 1 h by purging with Ar. All DU -0.75 Ti specimens were polished through 600-grit SiC paper and ultrasonically cleaned in acetone before immersion into the solution. Ion-implanted specimens were only ultrasonically cleaned in acetone without polishing. Polarization scans at a scan rate of 5 V/hr (1.39 mV/s) commenced

\* Contest Laboratories, Inc., Cypress, TX.

\*\* Army Materials Technology Laboratory, Watertown, MA 02172-0001.

<sup>†</sup> Trade name.

at  $E_{\text{corr}}$  after the samples were equilibrated in the solution for 1 h. All potentials were measured against a saturated calomel electrode (SCE).

### Surface analyses

Scanning electron microscopy (SEM) and EDS were performed on a JEOL<sup>†</sup> 840 microscope with a Tracor<sup>†</sup> Northern EDS attachment. A PHI<sup>†</sup> model 548 ESCA/Auger instrument was used for AES analysis. The spectra were taken at an electron voltage of 5 KeV. Sputtering was accomplished in an Ar atmosphere with a sputtering rate equivalent to the removal of 1000 Å of  $\text{Ta}_2\text{O}_5$  in 13 min. During sputtering, the peak-to-peak height of each element was recorded and converted to atomic concentration afterwards by taking the sensitivity factors into account.

## Results

### Electrochemical tests

**Acidic Solution.** The potentiodynamic polarization curves of DU -0.75 Ti and Mo-implanted DU -0.75 Ti in deaerated 1 N  $\text{H}_2\text{SO}_4$  (pH 1) are shown in Figure 1. The corrosion potential of the implanted specimen was about 300 mV more noble than that of the unimplanted DU. Passive regions without marked active-passive transitions were observed for both materials where the passive current densities (CDs) were in the range of 1 to 5  $\mu\text{A}/\text{cm}^2$ . There was no color change of the solution and little gas evolution was observed at the electrodes. The polarization curve for Mo/DU -0.75 Ti shows a peak at 370 mV, which probably results from the dissolution of Mo into the solution. The absence of another dissolution peak on successive scans (not shown in Figure 1) indicates that all Mo was probably dissolved during the initial scan.

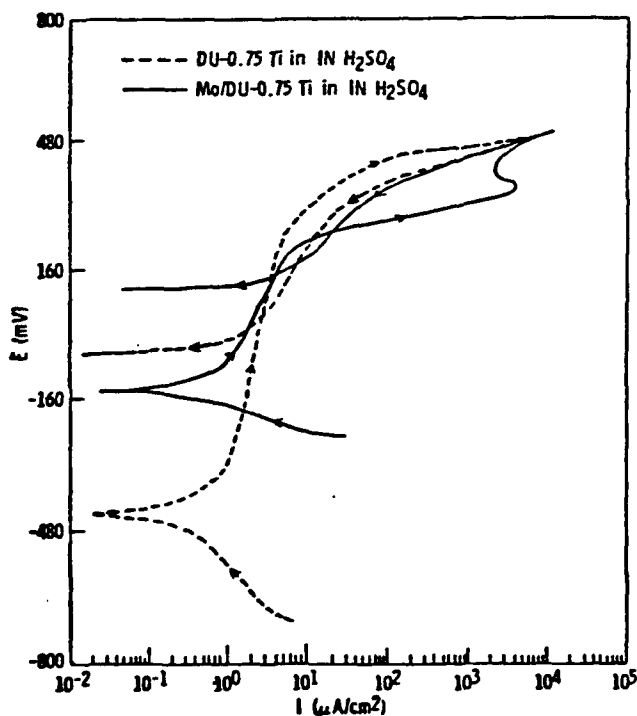


FIGURE 1 — Anodic polarization curves of DU -0.75 Ti and Mo/DU -0.75 Ti in deaerated 1 N  $\text{H}_2\text{SO}_4$  at room temperature.

<sup>†</sup> Trade name.

**Acidic Chloride Solutions.** The pitting corrosion potential ( $E_p$ ) of DU -0.75 Ti in acidic solutions was measured in 1 N  $\text{H}_2\text{SO}_4 + x$  ppm Cl. Cyclic polarization started at  $E_{\text{corr}}$  and was reversed when the CD reached either 1 or 10  $\text{mA}/\text{cm}^2$  in order to locate the pitting potential and the repassivation potential ( $E_{\text{rp}}$ ). For DU -0.75 Ti, the  $E_{\text{corr}}$  and the passivation CD increased slightly when the chloride concentration  $[\text{Cl}^-]$  increased from 0 to 150 ppm. When  $[\text{Cl}^-]$  was higher than 150 ppm, current fluctuations on the reverse scan were observed, suggesting that the passive film became unstable. When  $[\text{Cl}^-]$  was equal to 300 ppm, the reverse scan did not intercept the forward scan and crevice corrosion was observed after the experiment. Visual examination showed no evidence of pitting when the chloride concentration was 300 ppm and below, but pitting was observed when  $[\text{Cl}^-]$  was 400 and 500 ppm. Figure 2 shows the cyclic scans of DU -0.75 Ti in 1 N  $\text{H}_2\text{SO}_4 + 300, 400,$  and 500 ppm  $\text{Cl}^-$ . Also shown are duplicate polarization curves of implanted DU -0.75 Ti in 1 N  $\text{H}_2\text{SO}_4 + 400$  ppm  $\text{Cl}^-$  for comparison with those of the unimplanted specimen (only one curve of each specimen was shown). The implanted sample in duplicate scans had  $E_{\text{corr}}$  at 70 and 97 mV, which were about 550 mV more noble than the -470 mV of the unimplanted specimen. The Mo/DU -0.75 Ti also had  $E_p$  at 250 and 290 mV, which were 75 to 130 mV more noble than the 160 and 175 mV of the unimplanted specimen. The unimplanted DU -0.75 Ti did not repassivate even after a reverse scan to  $E_{\text{corr}}$ , while the implanted material repassivated at about +130 mV. When pitting occurred, a large amount of black powder, probably  $\text{UO}_2$  formed at the pits of both samples. The surface of MoDU was dark blue after the conclusion of the experiment. The unimplanted DU -0.75 Ti appeared to have larger pits, which might result from the longer pit growth period during the reverse scan. The implanted alloy repassivated quickly so there was little time for pits to grow.

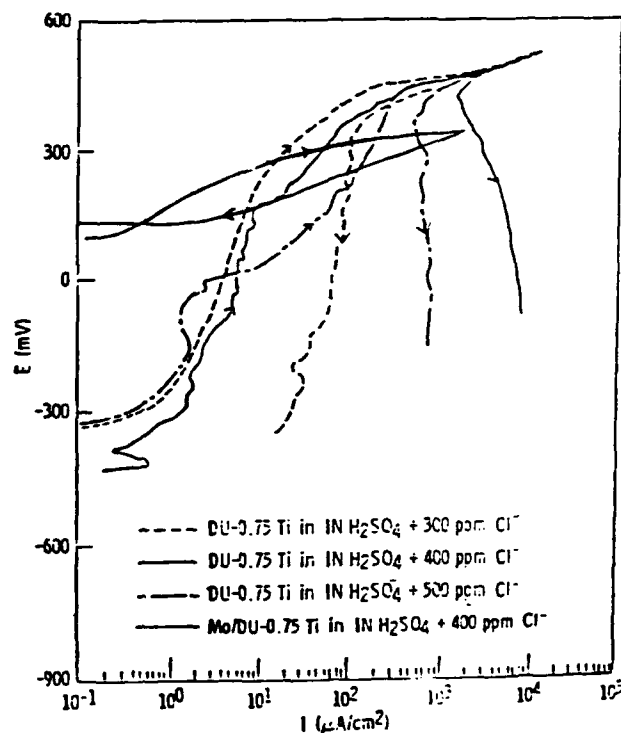


FIGURE 2 — Polarization curves of unimplanted and Mo-implanted DU -0.75 Ti in deaerated 1 N  $\text{H}_2\text{SO}_4 + 300, 400,$  and 500 ppm  $\text{Cl}^-$ .

**Neutral Chloride Solutions.** Unimplanted DU -0.75 Ti pitted readily in the neutral solution with a chloride concentration as low as 50 ppm and did not repassivate. In 50 ppm  $\text{Cl}^-$  solution, a limited passive region was observed, while in 0.005 M NaCl solution, the

current increased steadily from  $E_{\text{corr}}$ , and the anodic current was generally one magnitude greater. Gas bubbles were observed on the surface during scanning and pits were found after the experiment. Two pitting scans in 50 ppm  $\text{Cl}^-$  were performed on each specimen; the results are shown in Figure 3. The  $E_{\text{corr}}$  of Mo/DU -0.75 Ti was at least 50 mV more noble than the  $E_{\text{corr}}$  of DU -0.75 Ti; however, the CD of the implanted specimen was higher than that of the unimplanted specimen. The pitting potential of the implanted DU was 95 mV on one run and was difficult to define on the other run because no clear passive region could be found. The polarization curves of the unimplanted DU -0.75 Ti displayed two breakdown potentials, one at a low current level (1 to 2  $\mu\text{A}/\text{cm}^2$ ) and one at a higher current level (10 to 30  $\mu\text{A}/\text{cm}^2$ ). The low breakdown potential was 50 mV for both runs, while the higher breakdown potentials were 130 and 260 mV for both runs, respectively. The low breakdown potential may represent the first pit event; the higher breakdown potential may be related to secondary pitting. Repassivation was not observed on either specimen. Nonadherent black powder was again found on both pitted specimens, but pitting was more severe in the unimplanted alloy. This may have resulted in part from terminating the reverse scan early for the implanted alloy but running the gamut to  $E_{\text{corr}}$  for the unimplanted alloy.

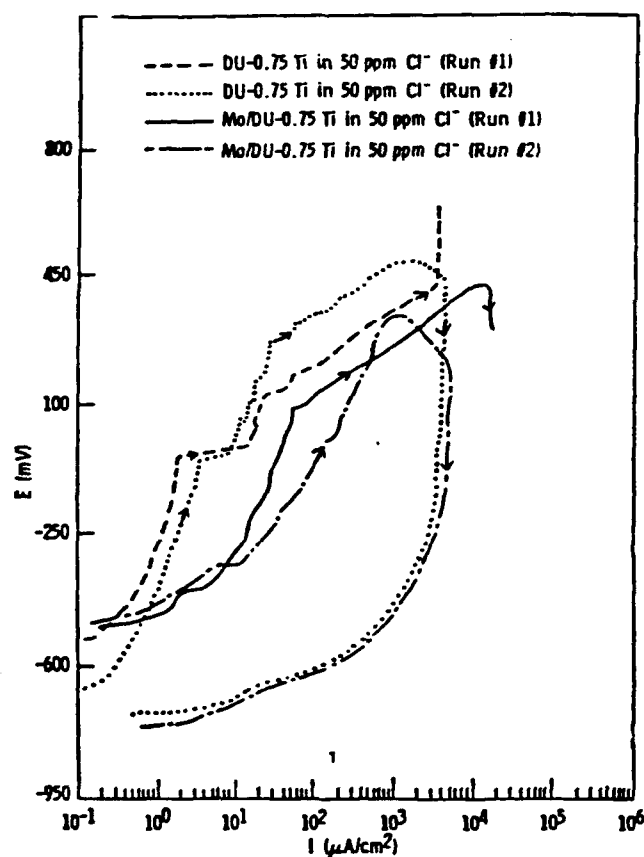


FIGURE 3 — Pitting scans of DU -0.75 Ti and Mo<sup>+</sup>-implanted DU -0.75 Ti in deaerated 50 ppm  $\text{Cl}^-$  solution.

**Alkaline Chloride Solutions.** The DU -0.75 Ti was much more resistant to pitting attack in NaOH than in  $\text{H}_2\text{SO}_4$  and neutral solutions. It did not pit in 1 N NaOH with up to 0.2 N NaCl added. Crevice corrosion was observed in 1 N NaOH + 0.5 N NaCl and 1 N NaOH + 1 N NaCl solutions. Pitting of DU -0.75 Ti in 0.5 N NaOH + 0.5 N NaCl occurred at 300 mV, as shown in Figure 4. The Mo-implanted specimen was much more resistant to pitting in this environment with a pitting potential at about 800 mV (Figure 4). On the other hand, the implanted sample had a lower  $E_{\text{corr}}$ , about 150

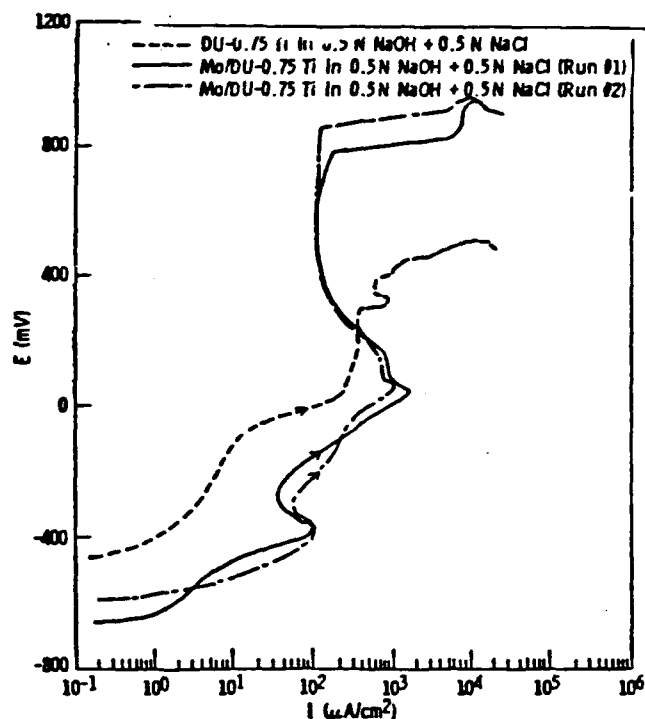


FIGURE 4 — Pitting scans of DU -0.75 Ti and Mo/DU -0.75 Ti in 0.5 N NaOH + 0.5 N NaCl solution.

to 200 mV lower, than the unimplanted alloy. Both specimens did not appear to repassivate, and the reverse scans were terminated at about 100 mV after reversal to avoid extensive uranium corrosion. Black powder was present around the pits.

### Surface analyses

**Electron Dispersive Spectroscopy.** EDS was used to determine the composition of the material in the pits and on the surface, before and after tests. However, because Ti was only 0.75 wt% in the bulk alloy, and the amount of Mo in the whole excitation volume (1 cu  $\mu\text{m}$ ) was very small, EDS did not provide conclusive results. In most cases, EDS showed that U is above 99%, while Ti and Mo are less than 0.5%, which was very close to the resolution limits of EDS. EDS mapping was attempted in order to identify the reaction products formed in the pits. Even distributions of Ti and Mo on the surface around the pits and in the pits were found by EDS mappings, which suggests that either no compounds of Ti or Mo were present in the pits, or that the concentrations of these elements were less than the detection limit of this technique (0.5 to 1%). Sodium chloride was identified on both DU -0.75 Ti and Mo/DU -0.75 Ti surfaces after experiments in the 0.5 N NaOH + 0.5 N NaCl solution.

**Auger Electron Spectroscopy.** AES analysis combined with Ar sputtering was used to generate the composition depth profiles of specimens before and after tests. Since the disk specimens were covered at the edges during polarization experiments, the outside protected region was analyzed as representative of the before-test condition. The central area exposed to the solution and subjected to electrochemical tests was considered the after-test condition.

(1) **Acidic solution.** The AES profile of the Mo<sup>+</sup>-implanted sample before test is shown in Figure 5. Mo is normally distributed under the surface instead of the anticipated Mo distribution (dotted line in Figure 5). The oxygen concentration decreases while the DU concentration increases continuously from the surface to the bulk. Both Mo and O peaks diminish after 10 to 15 min of sputtering, which suggests that almost all of the implanted Mo exists in the oxide, and very little Mo is in the bulk. The oxide thickness is approximately 1000 Å, estimated from sputtering of  $\text{Ta}_2\text{O}_5$  (1000 Å in 13 min of sputtering). The Mo concentration is about 5 at% (7 wt%) at the

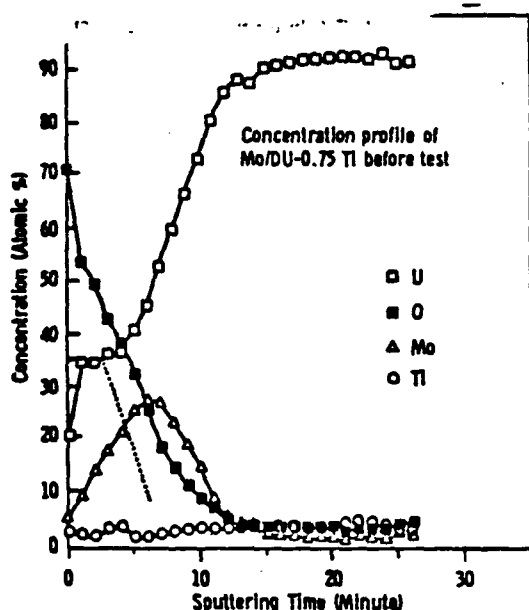


FIGURE 5 — Depth profile of AES on Mo<sup>+</sup>-implanted DU -0.75 Ti specimen before test. Dotted line represents the anticipated Mo concentration profile.

surface and reaches 27 at% (18 wt%) halfway into the oxide. After test, most of the Mo in the oxide disappeared (Figure 6); the highest Mo concentration was only about 10 at% and was distributed more evenly throughout the oxide (5 at%). The oxide thickness, however, remained the same.

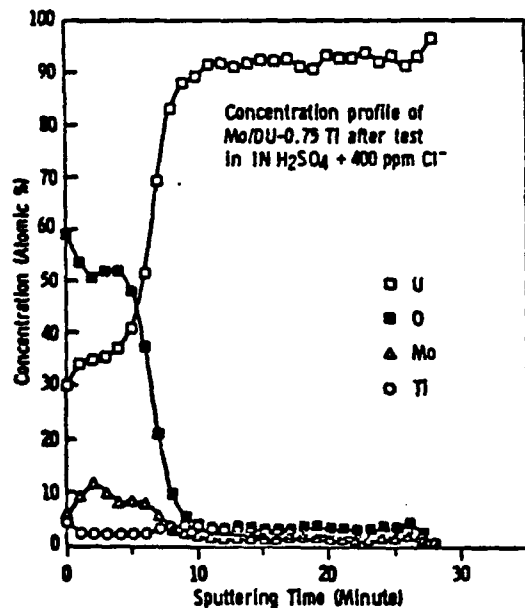


FIGURE 6 — AES depth profile of Mo<sup>+</sup>-implanted DU -0.75 Ti after test in 1 N H<sub>2</sub>SO<sub>4</sub> + 400 ppm Cl<sup>-</sup> solution.

(2) **Neutral solution.** The AES profile of the before-test specimen is very similar to the previous one, which indicates that the ion implantation process produces consistent results. The AES profile after test was also the same as that before test, i.e., the one shown in Figure 5. All Mo was still in the oxide and the oxide thickness did not change.

(3) **Alkaline solution.** For the Mo/DU -0.75 Ti tested in 0.5 N NaOH + 0.5 N NaCl solution, three profiles were taken: before test,

after test, and in the pit. The profile before test was the same as previous ones. After test, however, the oxide became very thick (Figure 7), such that after sputtering for 55 min, the oxygen concentration remained at 25 at%. This implies that the oxide film grew considerably during test (>3000 Å). The profile on the pit was similar to the one taken from the after test surface, i.e., low Mo concentration and thick oxide. The AES profile taken in the pit showed very low chloride concentration ≤(1 at%) throughout the oxide film. The fact that the Mo concentration was very low in both after test and in the pit profiles suggests that Mo disappeared during the test, and Mo compounds were not formed in the pits.

## Discussion

The effect of ion implantation on corrosion has been studied by several researchers,<sup>7,9-21</sup> and different mechanisms have been proposed. Ashworth and coworkers<sup>7</sup> suggested that ion implantation, *per se*, has very little or no effect on the corrosion properties of base materials; the implantation effect is similar to alloying in the base-metal solid solution. Al-Saffar, et al.,<sup>9</sup> explained the effect of Mo implantation on Al as either the incorporation of Mo into the Al passive film or dissolution and reprecipitation as some Mo-containing species on the film. Natishan, McCafferty, and Hubler<sup>20,21</sup> proposed a theory based on the concept of pH of zero charge to explain their results on the pitting resistance of implantation of Mo, Si, Nb, Zr, and Al on aluminum. Rubio and coworkers<sup>14</sup> thought the implantation effect comprises a mechanical effect, resulting from the structure change produced by implantation, and a chemical effect, resulting from the chemical nature of the implanted species. Implanted species have also been found by Walker and Chance<sup>19</sup> to thicken the passive film on steel and hence improve the film stability.

Improvement of the pitting corrosion resistance of steels by molybdenum alloying has been studied extensively.<sup>22</sup> Kolytyrkin and Knyazheva thought that Mo improves the stability of the passive film on stainless steels (SSs).<sup>23</sup> Molybdenum was shown by Hashimoro and coworkers to form compounds on active surface sites of ferritic SS and to reduce their activity.<sup>24</sup> Galvele, et al., proposed that the dissolution rate of a CrCl<sub>3</sub> salt layer on the surface of 18% Cr SS is reduced by Mo.<sup>25</sup> Sugimoto and Sawada suggested that Mo<sup>6+</sup> is present in the chromium oxyhydroxide on CrNiMo SS and improves its pitting resistance.<sup>26</sup> Ambrose found that a protective salt film containing Mo formed in the crevice of the FeMo alloys and resulted in repassivation of the crevice.<sup>27,28</sup> Ogawa and Sugimoto believed that the molybdenum in SSs forms molybdate in the solution and acts as an inhibitor for pitting corrosion.<sup>29,30</sup>

We propose a mechanism similar to that proposed by Ogawa and Sugimoto for molybdenum in SS,<sup>29,30</sup> namely that the implanted Mo dissolved into the solution and formed a molybdate that acted as an inhibitor to prevent or retard pitting initiation. This mechanism is explained in detail for the different environments, since our study showed that the effect of Mo-ion implantation on the pitting corrosion of DU -0.75 Ti depends very much on the pH of the solution.

## In alkaline solution

Molybdenum-ion implantation on DU -0.75 Ti markedly shifts the pitting potential in deaerated NaOH + NaCl solution (pH 14) in the noble direction. The implanted molybdenum dissolved into the solution as indicated by the decrease in Mo concentration in the oxide film after testing (Figure 7). From the potential-pH diagram<sup>31</sup> molybdenum forms molybdate in aqueous solution when pH > 6. Molybdate has long been used as a corrosion inhibitor for both ferrous and nonferrous metals.<sup>32-36</sup> Generally, oxygen must be present in solution for the molybdate to be effective,<sup>32</sup> but Björmi and Gabe found that aeration is not necessary for molybdate to inhibit the corrosion of zinc.<sup>36</sup> Furthermore, it has been recently found that sodium molybdate inhibits uniform corrosion and reduces the passive CD of DU -0.75 Ti and DU -2Mo in deaerated NaF and NH<sub>4</sub>HF<sub>2</sub> solutions.<sup>37</sup>

To confirm our proposed mechanism, polarization experiments



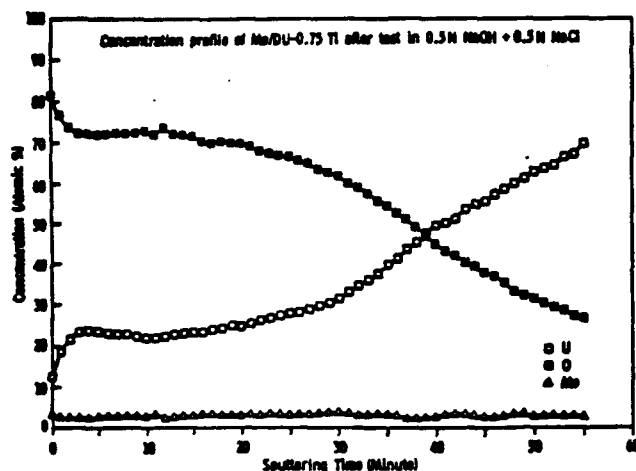


FIGURE 7 — AES depth profile of Mo<sup>+</sup>-implanted DU-0.75 Ti after pitting scan in 0.5 N NaOH + 0.5 N NaCl solution.

were conducted for unimplanted DU-0.75 Ti in deaerated 0.5 N NaOH + 0.5 N NaCl + 0.1 M and 0.2 M Na<sub>2</sub>MoO<sub>4</sub> solutions and compared to those for the Mo-implanted alloy in the same environment but without molybdate. The pitting potentials of DU-0.75 Ti in the molybdate-containing solutions are 1350 and 1420 mV, respectively, as shown in Figure 8. They are at least 110 mV more noble than the E<sub>p</sub> in the same solution without molybdate (Figure 8). Figure 8 also shows that the polarization curves of Mo<sup>+</sup>-implanted DU-0.75 Ti in 0.5 N NaOH + 0.5 N NaCl and DU-0.75 Ti in 0.5 N NaOH + 0.5 N NaCl + 0.1 M Na<sub>2</sub>MoO<sub>4</sub> are very similar. The passive CD's are around 10 μA/cm<sup>2</sup>. The peaks on the polarization curve of Mo/DU-0.75 Ti at about -400 and 100 mV may be related to the dissolution of molybdenum. The total amount of Mo implantation is very small, about 10<sup>17</sup> ions/cm<sup>2</sup>; the dissolved Mo is even less. Hence, it is very difficult to detect the dissolved Mo in the solution. Calculations show that if the dissolved Mo is evenly distributed in the solution, the molybdate concentration is approximately 100 ppb. In an unstirred solution, the molybdate concentration would be higher than 10 ppb near the specimen surface but would not reach a concentration of 0.1 or 0.2 M. This explains why the Mo/DU-0.75 Ti has a lower pitting potential than the DU-0.75 Ti in the same solution with 0.1 or 0.2 M sodium molybdate.

Kodama and Ambrose detected Mo in the pits on iron after exposure in Cl<sup>-</sup> and Na<sub>2</sub>MoO<sub>4</sub> solution and concluded that molybdenum forms an insoluble film and retarded pit growth.<sup>28</sup> But this mechanism is not operative in the case of the DU-0.75 Ti alloy because there is little or no Mo compound formed in the pits. In our case, the implanted Mo dissolves and forms MoO<sub>4</sub><sup>2-</sup> in the solution, then the molybdate is preferentially absorbed on the surface in competition with Cl<sup>-</sup>, thereby reducing the surface Cl<sup>-</sup> concentration, and pit initiation is retarded.

The extensive growth of passive oxide film during the polarization experiments with the Mo-implanted alloy is thought to be a result of the molybdate inhibition that retarded pitting and extended the passive region. The implanted DU-0.75 has a corrosion potential 150 to 200 mV more active than the unimplanted alloy. But adding 0.1 M or 0.2 M Na<sub>2</sub>MoO<sub>4</sub> to the solution has very little effect on the corrosion potential of the unimplanted DU-0.75 Ti. The more electronegative potential of the implanted alloy cannot be accounted for by the formation of molybdate but probably results from the effect of alloying the surface with molybdenum.<sup>1</sup>

#### In neutral solution

Mo/DU-0.75 Ti has a higher passive CD and a lower E<sub>p</sub> than the breakdown potential of the unimplanted DU-0.75 Ti. In other words, the Mo implantation does not improve the pitting resistance

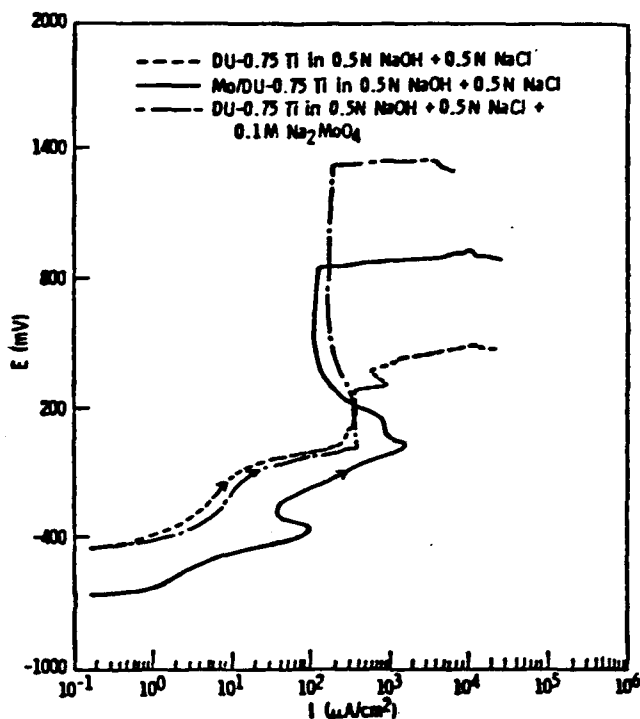


FIGURE 8 — Polarization scans of Mo/DU-0.75 Ti and DU-0.75 Ti in 0.5 N NaOH + 0.5 N NaCl and DU-0.75 Ti in 0.5 N NaOH + 0.5 N NaCl + 0.1 M Na<sub>2</sub>MoO<sub>4</sub>.

of DU-0.75 Ti. Thus, it was initially believed that molybdate would not have an inhibiting effect in neutral chloride solution. But adding (0.2 M or 0.1 M) molybdate to 50 ppm Cl<sup>-</sup> solution does shift the pitting potential of unimplanted DU-0.75 Ti in the more noble direction (Figure 9). In 50 ppm Cl<sup>-</sup> + 0.1 M Na<sub>2</sub>MoO<sub>4</sub> solution, DU-0.75 Ti has an E<sub>p</sub> of +250 mV, which is 200 mV more noble than the alloy in the same solution without molybdate. It repassivates at an E<sub>rp</sub> of -10 mV in 50 ppm Cl<sup>-</sup> + 0.1 M Na<sub>2</sub>MoO<sub>4</sub> compared to no repassivation in 50 ppm Cl<sup>-</sup> without Na<sub>2</sub>MoO<sub>4</sub>. This indicates that molybdate should inhibit pitting of DU-0.75 Ti in neutral chloride solution. But in the case of the Mo-implanted alloy, Auger analysis showed that the Mo concentration in the passive film did not decrease after test. Therefore, Mo did not go into solution. MoO<sub>4</sub><sup>2-</sup> was not formed, and inhibition was not observed. An explanation for the absence of Mo dissolution (within the limits of the AES data) is that the pitting potential of DU-0.75 Ti in this environment is so close to the E<sub>corr</sub> that pitting occurs before Mo dissolves.

MoO<sub>2</sub> can be formed in neutral and slightly acid environments according to the potential-pH diagram for molybdenum.<sup>31</sup> If MoO<sub>2</sub> does form during test, the oxygen concentration in the after test AES profile will increase and molybdenum concentration will decrease. But this behavior was not observed, and we concluded that no MoO<sub>2</sub> was formed.

#### In acidic solution

The role of molybdate in the acid environment is very complex, as reported previously by other researchers.<sup>31,32,34</sup> At pH below 3, three species MoO<sub>2</sub>, MoO<sub>3</sub> · H<sub>2</sub>O, or MoO<sub>2</sub><sup>2+</sup>, according to Vukosorich and Farr,<sup>32</sup> or MoO<sub>2</sub>, MoO<sub>2</sub><sup>2+</sup>, or Mo<sub>2</sub>O<sub>7</sub><sup>2-</sup>, according to Pourbaix,<sup>31</sup> could form depending on the pH. The condensed isopolymolybdates or their hydrolysis products, heteropolymolybdates, do have an inhibiting effect on steels in acid solutions.<sup>34,38-42</sup> In acidic solution, sodium molybdophosphate is a passivating agent that does not significantly change the anodic characteristics of AISI 4340 steel, according to Lizlovs.<sup>38</sup> But Stranick reported that molybdate is less effective on mild steel in acidic than in neutral and basic solutions.<sup>34</sup>

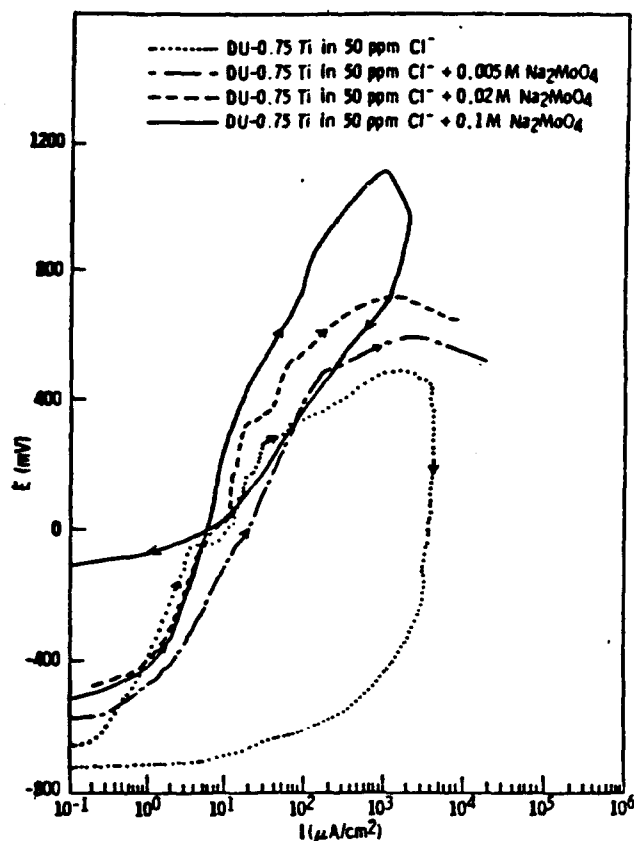


FIGURE 9 — Pitting scans of DU -0.75 Ti in 50 ppm  $\text{Cl}^-$  + 0 M, 0.005 M, 0.02 M, and 0.1 M  $\text{Na}_2\text{MoO}_4$  solutions.

The  $\text{Mo}^+$  implantation markedly shifts the corrosion potential of DU -0.75 Ti in the noble direction and also increases (more noble) the pitting potential in 1 N  $\text{H}_2\text{SO}_4$  + 400 ppm  $\text{Cl}^-$  solution (Figure 2). The AES depth profile shows that the concentration of implanted Mo decreased after test, probably a result of dissolution of Mo. The surface of Mo/DU -0.75 Ti after exposure in the acid solution became blue. The blue film on the surface could be the deposition of iso- or heteropolymolybdates that formed after the implanted Mo dissolved into the solution. This deposit on the surface would increase the corrosion potential as well as the pitting potential of DU -0.75 Ti. A polarization experiment was attempted on DU -0.75 in deaerated 1 N  $\text{H}_2\text{SO}_4$  + 400 ppm  $\text{Cl}^-$  + 0.1 M  $\text{Na}_2\text{MoO}_4$  solution to simulate the effect of molybdate. But at the open-circuit potential, the specimen started to pit in less than 10 min. The area around the pits became dark blue and expanded as pits grew. When the specimen was taken out of the solution, the dark blue regions that appeared as fine particles covered the whole specimen surface. The specimen was examined by EDS and Mo was found on the surface and was more concentrated on the corrosion products. Further investigation is needed to understand this phenomenon. Glass<sup>43</sup> reported that a Mo salt film replaces  $\text{TiO}_2$  on Ti in deaerated 1 N  $\text{H}_2\text{SO}_4$ . But in our study, no comparable replacement of Mo for  $\text{UO}_2$  can be confirmed.

In summary,  $\text{Mo}^+$  implantation is only effective against pitting corrosion of DU -0.75 Ti when the molybdenum is dissolved from the surface into solution. After dissolution, it forms a molybdate and behaves like a pitting inhibitor. Without Mo dissolution,  $\text{Mo}^+$  implantation does not improve the pitting resistance of DU -0.75 Ti

### Conclusion

The unimplanted DU -0.75 Ti is more resistant to pitting corrosion in 0.5 N  $\text{NaOH}$  than in 1 N  $\text{H}_2\text{SO}_4$  solutions. It is most susceptible to pitting in neutral chloride solution. The beneficial effect of  $\text{Mo}^+$  implantation against pitting was found in acidic and

alkaline chloride solutions but not in neutral chloride solution. A mechanism based on the dissolution of implanted molybdenum and the formation of molybdates is proposed to account for the corrosion inhibition.

(1) In alkaline chloride solution, molybdate formed after Mo dissolved from the surface oxide. The molybdate then preferentially absorbed on the surface to reduce the surface chloride ion concentration with concomitant reduction of susceptibility to pitting.

(2) In neutral solution, there was no evidence of Mo dissolution and molybdate formation. Since inhibition was not observed, it is suggested that implanted Mo will not inhibit pitting unless it is dissolved. The reason that Mo did not dissolve is probably because the corrosion potential and the pitting potential of DU -0.75 Ti are so close that the specimen pits before Mo dissolves.

(3) In acidic solution, the implanted Mo dissolved and formed a blue complex of polymolybdates that deposited on the surface. This deposition would slow down the chloride attack. As a consequence, the pitting potential shifts in the noble direction.

### Acknowledgment

The authors express their gratitude to B. D. Sartwell of the Navy Research Laboratory for the ion implantation work and to S.-S. Lin, Ph.D., of the Army Materials Technology Laboratory (AMTL) for the Auger analyses.

### References

1. M. Levy, C. V. Zabielski, *Physical Metallurgy of Uranium Alloys*, J. J. Burke, D. A. Colling, A. E. Gorum, J. Greenspan, Eds., p. 897, 1974.
2. J. T. Waber, *Proc. of 2nd U.S. International Conference on Peaceful Use of Atomic Energy*, Vol. 6, p. 204, 1958.
3. J. M. Macki, R. L. Kochen, *Nucl. Sci. Abst.*, Vol. 25, No. 14, p. 326, 1971.
4. J. W. Dini, H. R. Johnson, *Metal Finishing*, Vol. 45, No. 6, 1963.
5. L. J. Weirick, *Physical Metallurgy of Uranium Alloys*, J. J. Burke, D. A. Colling, A. E. Gorum, J. Greenspan, Eds., p. 949, 1974.
6. L. J. Weirick, D. L. Douglass, *Corrosion*, Vol. 32, No. 6, p. 209, 1976.
7. V. Ashworth, R. P. M. Procter, W. A. Grant, *Treatise on Materials Science and Technology*, J. K. Hirvonen, Ed., Academic Press, Vol. 18, p. 175, 1980.
8. A. M. Ammons, *Physical Metallurgy of Uranium Alloys*, J. J. Burke, D. A. Colling, A. E. Gorum, J. Greenspan, Eds., p. 511, 1974.
9. A. H. Al-Saffar, V. Ashworth, A. K. O. Barramov, D. J. Chivers, W. A. Grant, R. P. Procter, *Corr. Sci.*, Vol. 20, p. 127, 1980.
10. F. C. Chang, M. Levy, S. S. Lin, *CORROSION 85*, Paper No. 71, National Association of Corrosion Engineers, Houston, TX, 1985.
11. C. R. Clayton, Y. F. Wang, G. K. Hubler, *Passivity of Metals and Semiconductors*, M. Froment, Ed., Elsevier Science, Amsterdam, The Netherlands, p. 115, 1983.
12. R. Viorri, D. Popgoshchev, G. K. Hubler, *Passivity of Metals and Semiconductors*, M. Froment, Ed., Elsevier Science, Amsterdam, The Netherlands, p. 152, 1983.
13. E. McCafferty, G. K. Hubler, J. K. Hirvonen, 1978 Tri-Service Conference on Corrosion, p. 435, 1979.
14. J. D. Rubio, R. R. Har, R. B. Griffin, *Corrosion*, Vol. 42, No. 9, p. 557, 1986.
15. F. A. Smidy, *NRL Memorandum Report 5*, p. 159, 1986.
16. M. V. Zeller, W. T. Eihara, *U.S. Army Armament R&D Center Contractor Report ARSCD-CR-83017*.
17. R. Wang, J. L. Brimhall, *Ion Implantation and Ion Beam Processing of Materials*, MRS Symposium Proceedings, Vol. 27, G. K. Hubler, O. W. Holl, C. R. Clayton, C. W. White, Eds., p. 729, 1985.
18. J. M. Williams, G. M. Beardsley, R. A. Buchanan, R. K. Bacon, *Ion Implantation, Ion Beam Processing of Materials*, MRS Symposium Proceedings, Vol. 27, G. K. Hubler, O. W. Holland,

- C. R. Clayton, C. W. White, Eds., p. 735, 1985.
19. M. S. Walker, R. L. Chance, Corrosion, 40, No. 6, p. 307, 1984.
  20. P. M. Natishan, E. McCafferty, G. K. Hubler, J. Electrochem Soc., 133, No. 15, p. 1061, 1986.
  21. E. McCafferty, Corrosion Prevention and Control, Proceedings of the 33rd Sagamore Conference, M. Levy, S. Isserow, Ed., p. 344, 1986.
  22. Z. Szklarska-Smialowska, Pitting Corrosion of Metals, NACE, Houston, TX, p. 143, 1986.
  23. Ya. M. Kolotykn, W. M. Knyazneva, Passivity of Metals, R. Frankenthal, J. Kruger, Eds., The Electrochemical Society Inc., Pennington, NJ, p. 678, 1978.
  24. K. Hashimoto, K. Asami, K. Teramoto, Corr. Sci., Vol. 19, p. 3, 1979.
  25. J. R. Gulvele, J. B. Lumsden, R. W. Staehle, J. Electrochem Soc., Vol. 125, p. 1204, 1978.
  26. K. Sugimoto, Y. Sawada, Corr. Sci., Vol. 17, p. 425, 1977.
  27. J. R. Ambrose Corrosion, Vol. 34, No. 1, p. 27, 1978.
  28. T. Kodama, J. R. Ambrose, Corrosion, Vol. 33, No. 5, p. 155, 1977.
  29. H. Ogawa, H. Omata, I. Itoh, H. Okada, Corrosion, Vol. 34, No. 2, p. 53, 1978.
  30. K. Sugimoto, Y. Sawada, Corrosion, Vol. 32, No. 9, p. 347, 1976.
  31. M. Pourbaix, Atlas of Electrochemical Equilibria in Aqueous Solutions, p. 272, NACE, Houston, TX, 1974.
  32. M. S. Vukasovich, J. P. G. Farr, Materials Performance, Vol. 25, No. 5, p. 9, 1986.
  33. D. R. Robitaille, Chem. Eng., No. 20, p. 139, 1982.
  34. M. A. Stranick, Corrosion, Vol. 40, No. 6, p. 296, 1984.
  35. E. A. Lizlovs, Corrosion, Vol. 32, No. 7, p. 263, 1976.
  36. D. Bijimi, D. R. Gabe, Br. Corr. J., Vol. 18, p. 138, 1983.
  37. C. Zabielski, J. Scanlon, unpublished data.
  38. E. A. Lizlovs, J. Electrochem Soc., Vol. 114, p. 1015, 1967.
  39. K. Ogura, T. Majima, Electrochem. Acta, Vol. 24, p. 325, 1979.
  40. J. N. Wanklyn, Corr. Sci., Vol. 21, No. 3, p. 211, 1981.
  41. K. Ogura, T. Ohama, Corrosion, Vol. 40, No. 2, p. 47, 1984.
  42. G. H. Cartledge, R. F. Sympton, J. Phys. Chem., Vol. 61, p. 973, 1957.
  43. R. S. Glass, Corrosion, Vol. 41, No. 2, p. 89, 1985.

DTIC QUALITY INSPECTED 3

Accession For	
NTIS GRA&I	<input checked="" type="checkbox"/>
DTIC TAB	<input type="checkbox"/>
Unannounced	<input type="checkbox"/>
Justification	
By	
Distribution/	
Availability Codes	
Dist	Avail and/or Special
A-1	20

# DISTRIBUTION LIST

No. of Copies	To
1	Office of the Under Secretary of Defense for Research and Engineering, The Pentagon, Washington, DC 20301
	Director, U.S. Army Research Laboratory, 2800 Powder Mill Road, Adelphi, MD 20783-1197
1	ATTN: AMSRL-OP-CI-AD, Technical Publishing Branch
1	AMSRL-OP-CI-AD, Records Management Administrator
	Commander, Defense Technical Information Center, Cameron Station, Building 5, 5010 Duke Street, Alexandria, VA 22304-6145
2	ATTN: DTIC-FDAC
1	MIA/CINDAS, Purdue University, 2595 Yeager Road, West Lafayette, IN 47905
	Commander, Army Research Office, P.O. Box 12211, Research Triangle Park, NC 27709-2211
1	ATTN: Information Processing Office
	Commander, U.S. Army Materiel Command, 5001 Eisenhower Avenue, Alexandria, VA 22333
1	ATTN: AMCSCI
	Commander, U.S. Army Materiel Systems Analysis Activity, Aberdeen Proving Ground, MD 21005
1	ATTN: AMXSY-MP, H. Cohen
	Commander, U.S. Army Missile Command, Redstone Arsenal, AL 35809
1	ATTN: AMSMI-RD-CS-R/Doc
	Commander, U.S. Army Armament, Munitions and Chemical Command, Dover, NJ 07801
2	ATTN: Technical Library
	Commander, U.S. Army Natick Research, Development and Engineering Center, Natick, MA 01760-5010
1	ATTN: Technical Library
	Commander, U.S. Army Satellite Communications Agency, Fort Monmouth, NJ 07703
1	ATTN: Technical Document Center
	Commander, U.S. Army Tank-Automotive Command, Warren, Mi 48397-5000
1	ATTN: AMSTA-ZSK
1	AMSTA-TSL, Technical Library
	Commander, White Sands Missile Range, NM 88002
1	ATTN: STEWS-WS-VT
	President, Airborne, Electronics and Special Warfare Board, Fort Bragg, NC 28307
1	ATTN: Library
	Director, U.S. Army Research Laboratory, Aberdeen Proving Ground, MD 21005
1	ATTN: AMSRL-WT
	Commander, Dugway Proving Ground, UT 84022
1	ATTN: Technical Library, Technical Information Division
	Commander, U.S. Army Research Laboratory, 2800 Powder Mill Road, Adelphi, MD 20783
1	ATTN: AMSRL-SS
	Director, Benet Weapons Laboratory, LCWSL, USA AMCCOM, Watervliet, NY 12189
1	ATTN: AMSMC-LCB-TL
1	AMSMC-LCB-R
1	AMSMC-LCB-RM
1	AMSMC-LCB-RP
	Commander, U.S. Army Foreign Science and Technology Center, 220 7th Street, N.E., Charlottesville, VA 22901-5396
3	ATTN: AIFRTC, Applied Technologies Branch, Gerald Schlesinger

No. of  
Copies

To

1 U.S. Army Aviation Training Library, Fort Rucker, AL 36360  
ATTN: Building 5906-5907

1 Commander, U.S. Army Agency for Aviation Safety, Fort Rucker, AL 36362  
ATTN: Technical Library

1 Commander, Clarke Engineer School Library, 3202 Nebraska Ave., N, Ft. Leonard Wood, MO 65473-5000  
ATTN: Library

1 Naval Research Laboratory, Washington, DC 20375  
ATTN: Technical Library

1 Mr. B. Sartwell - Code 6075

1 Chief of Naval Research, Arlington, VA 22217  
ATTN: Code 1131 Dr. J. Sedriks

1 Commander, U.S. Air Force Wright Research & Development Center,  
Wright-Patterson Air Force Base, OH 45433-6523

1 ATTN: WRDC/MLLP, M. Forney, Jr.

1 WRDC/MLBC, Mr. Stanley Schulman

1 Technical Library

1 NASA - Marshall Space Flight Center, MSFC, AL 35812  
ATTN: Mr. Paul Schuerer/EH01

1 Technical Library

1 U.S. Department of Commerce, National Institute of Standards and Technology, Gaithersburg, MD 20899  
ATTN: Chief, Metals Division, Institute for Materials Science and Engineering

1 Technical Library

1 Committee on Marine Structures, Marine Board, National Research Council, 2101 Constitution Avenue, N.W.,  
Washington, DC 20418

1 Materials Sciences Corporation, Suite 250, 500 Office Center Drive, Fort Washington, PA 19034

1 Charles Stark Draper Laboratory, 555 Technology Square, Cambridge, MA 02139

1 Wyman-Gordon Company, Worcester, MA 01601  
ATTN: Technical Library

1 General Dynamics, Convair Aerospace Division P.O. Box 748, Forth Worth, TX 76101  
ATTN: Mfg. Engineering Technical Library

1 NASA - Langley Research Center, Hampton, VA 23665-5225

1 U.S. Army Vehicle Propulsion Directorate, NASA Lewis Research Center, 2100 Brookpark Road,  
Cleveland, OH 44135-3191

1 ATTN: AMSRL-VP

1 NASA - Lewis Research Center, 2100 Brookpark Road, Cleveland, OH 44135-3191  
ATTN: Technical Library

1 Director, Defense Intelligence Agency, Washington, DC 20340-6053  
ATTN: ODT-5A (Mr. Frank Jaeger)

1 Commander, U.S. Army Research, Development and Engineering Center, Picatinny Arsenal, NJ 07806-5000  
ATTN: Technical Library

1 SMCAR-AET-M, Dr. B. Lakshminarayan

1 SMCAR-AET-E, Mr. A. Daniels

1 Dr. H. Shih, President, Cortech Corp., 14145 Proctor Ave., No. 14, City of Industry, CA 91746

1 Naval Post Graduate School, Monterey, CA 93948  
ATTN: Technical Library

1 Naval Surface Weapons Center, Dahlgren Laboratory, Dahlgren, VA 22448  
ATTN: Technical Library

No. of Copies	To
1	Commander, Rock Island Arsenal, Rock Island, IL 61299 ATTN: Technical Library
1	Georgia Institute of Technology, Atlanta, GA 30332 ATTN: Library
1	Kennemetal, Inc., P.O. Box 231, Latrobe, PA 15650 ATTN: Technical Library
2	Director, U.S. Army Research Laboratory, Watertown, MA 02172-0001 ATTN: AMSRL-OP-CI-D, Technical Library
15	Authors